

Supporting Information

Amphiphilic Guanidine-based Lipids Enhance mRNA Delivery and Immune Activation

Qi Wei^a, Ruoshui Li^a, Jiaqi Fan^a, Mengyuan Xu^a, Pengcheng Yuan^a, Jiwei Liu^a, Qian Wang^a, Youqing Shen^a, Nigel K. H. Slater^a, Jianbin Tang^{*a}.

^aZhejiang Key Laboratory of Smart Biomaterials, Key Laboratory of Biomass Chemical Engineering of Ministry of Education, College of Chemical and Biological Engineering, Zhejiang University, Hangzhou 310058, China

*Corresponding author: Jianbin Tang. Email: jianbin@zju.edu.cn

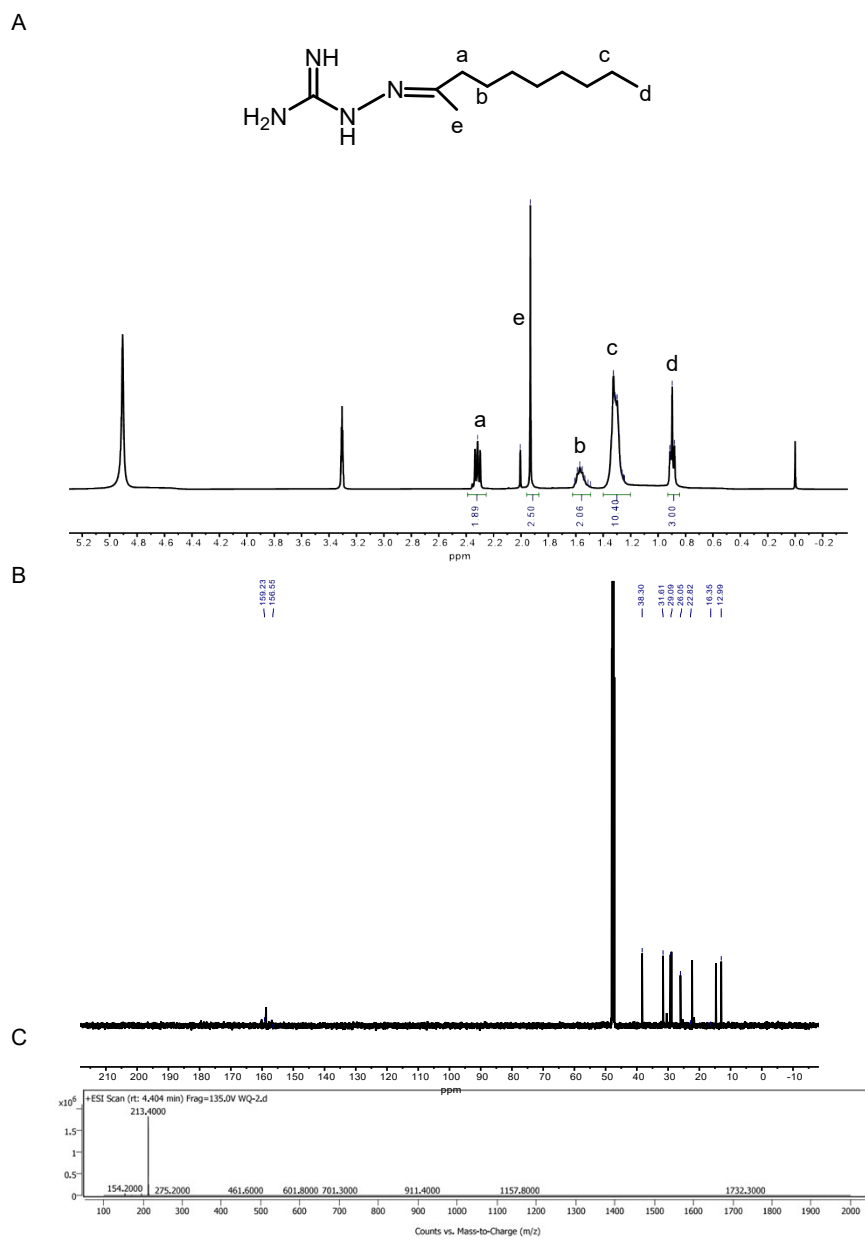


Figure S1 (A) The ^1H NMR spectrum of GL1 in CD_3OD . (B) The ^{13}C NMR spectrum of GL2 in CD_3OD .

(C) ESI-MS: m/z calculated for $\text{C}_{11}\text{H}_{24}\text{N}_4$ $[\text{M} + \text{H}]^+$: 212.2; found: 213.4.

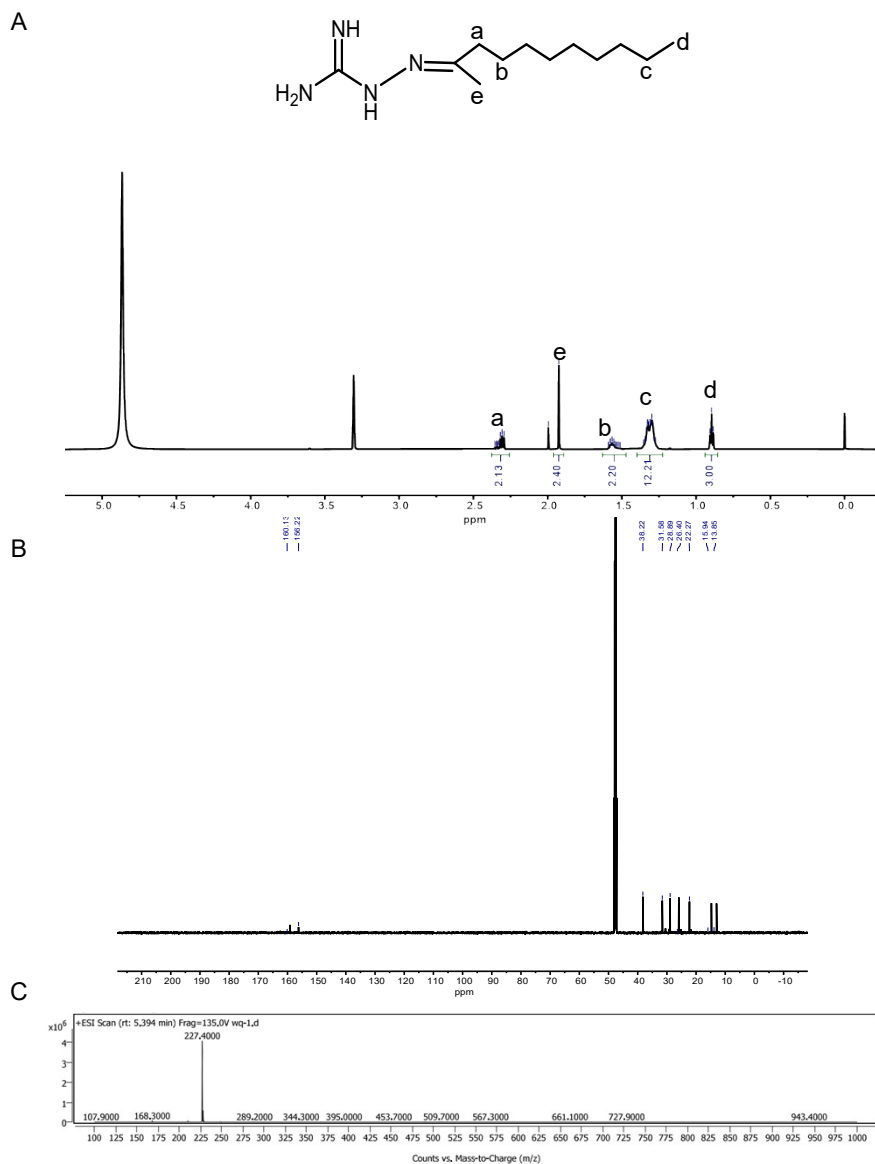
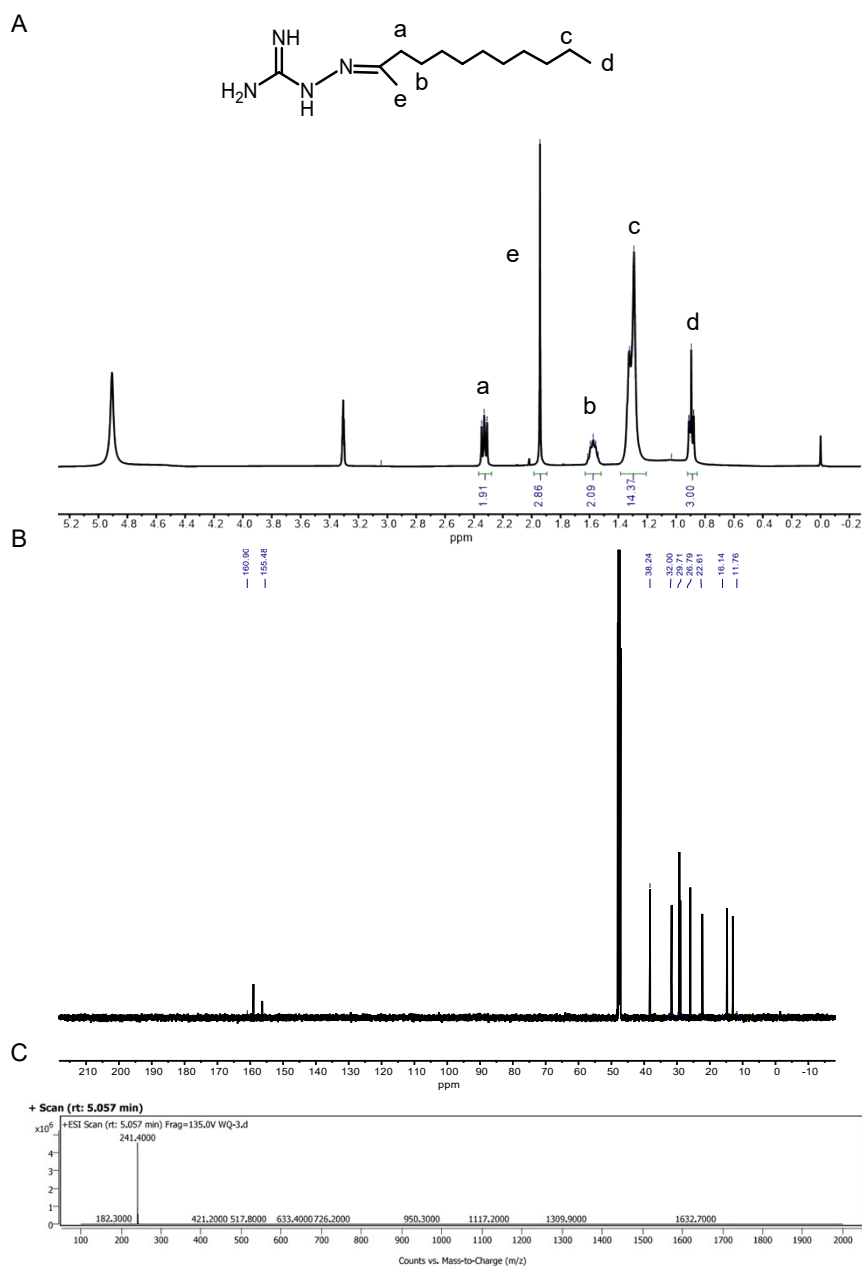


Figure S2 (A) The ^1H NMR spectrum of GL2 in CD_3OD . (B) The ^{13}C NMR spectrum of GL2 in CD_3OD .

(C) ESI-MS: m/z calculated for $\text{C}_{12}\text{H}_{26}\text{N}_4$ $[\text{M} + \text{H}]^+$: 226.22; found: 227.4.



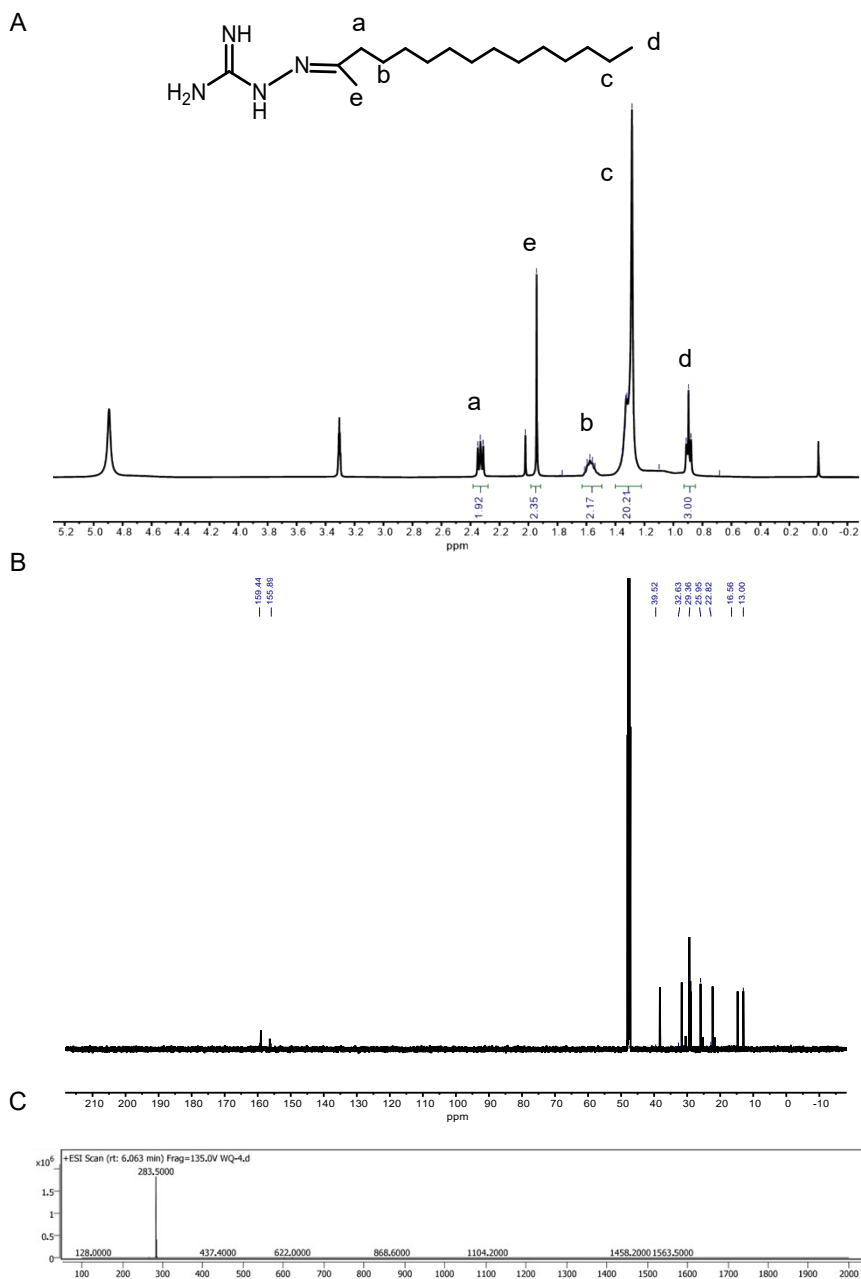


Figure S4 (A) The ^1H NMR spectrum of GL4 in CD_3OD . (B) The ^{13}C NMR spectrum of GL4 in CD_3OD . (C) ESI-MS: m/z calculated for $\text{C}_{16}\text{H}_{34}\text{N}_4$ $[\text{M} + \text{H}]^+$: 283.28; found: 283.5.

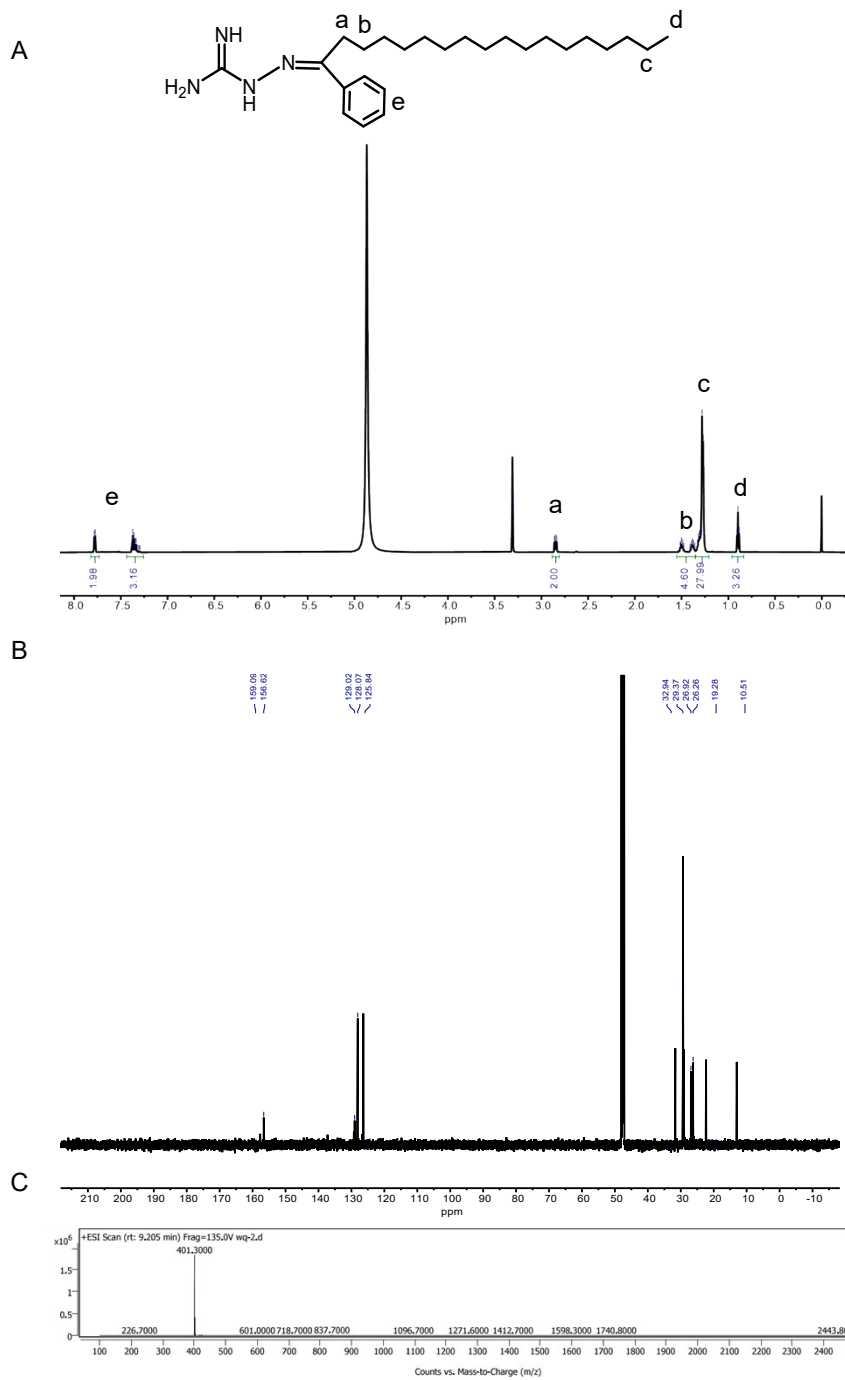


Figure S5 (A) The ^1H NMR spectrum of GL5 in CD_3OD . (B) The ^{13}C NMR spectrum of GL5 in CD_3OD .

(C) ESI-MS: m/z calculated for $\text{C}_{25}\text{H}_{44}\text{N}_4$ $[\text{M} + \text{H}]^+$: 401.66; found: 401.3.

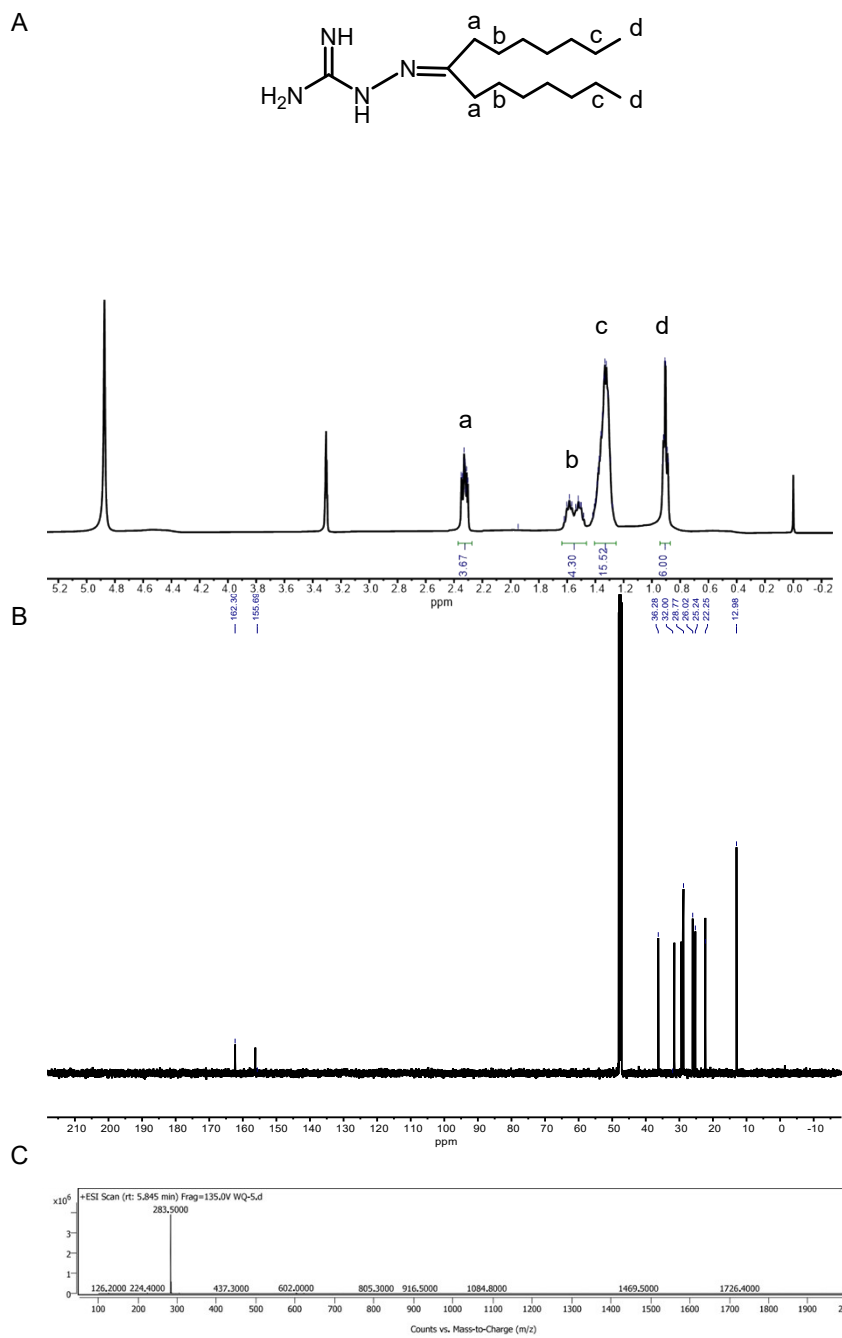


Figure S6 (A) The ^1H NMR spectrum of GL6 in CD_3OD . (B) The ^{13}C NMR spectrum of GL6 in CD_3OD .

(C) ESI-MS: m/z calculated for $\text{C}_{16}\text{H}_{34}\text{N}_4$ $[\text{M} + \text{H}]^+$: 283.28; found: 283.5.

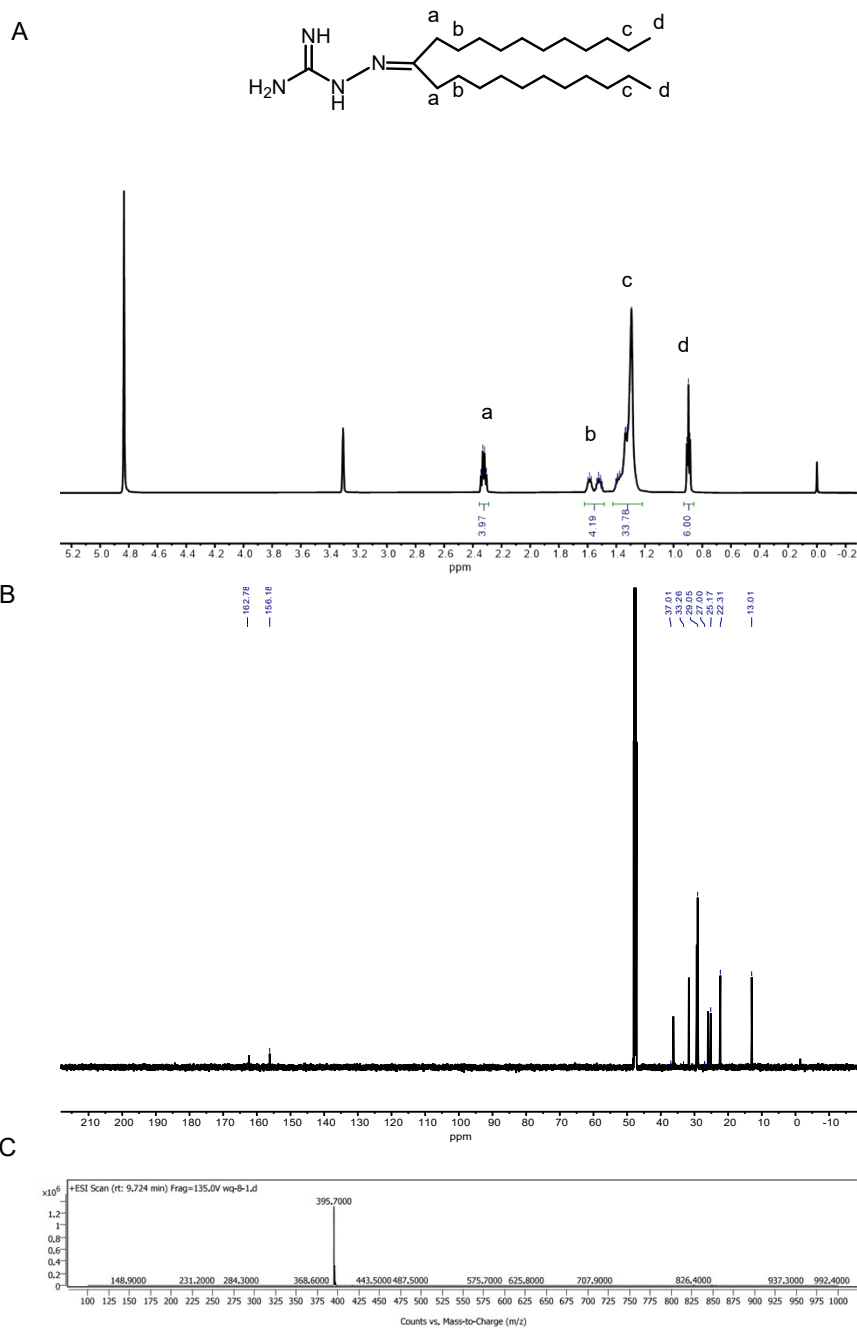


Figure S7 (A) The ^1H NMR spectrum of GL7 in CD_3OD . (B) The ^{13}C NMR spectrum of GL7 in CD_3OD . (C) ESI-MS: m/z calculated for $\text{C}_{24}\text{H}_{50}\text{N}_4$ $[\text{M} + \text{H}]^+$: 394.4; found: 395.7.

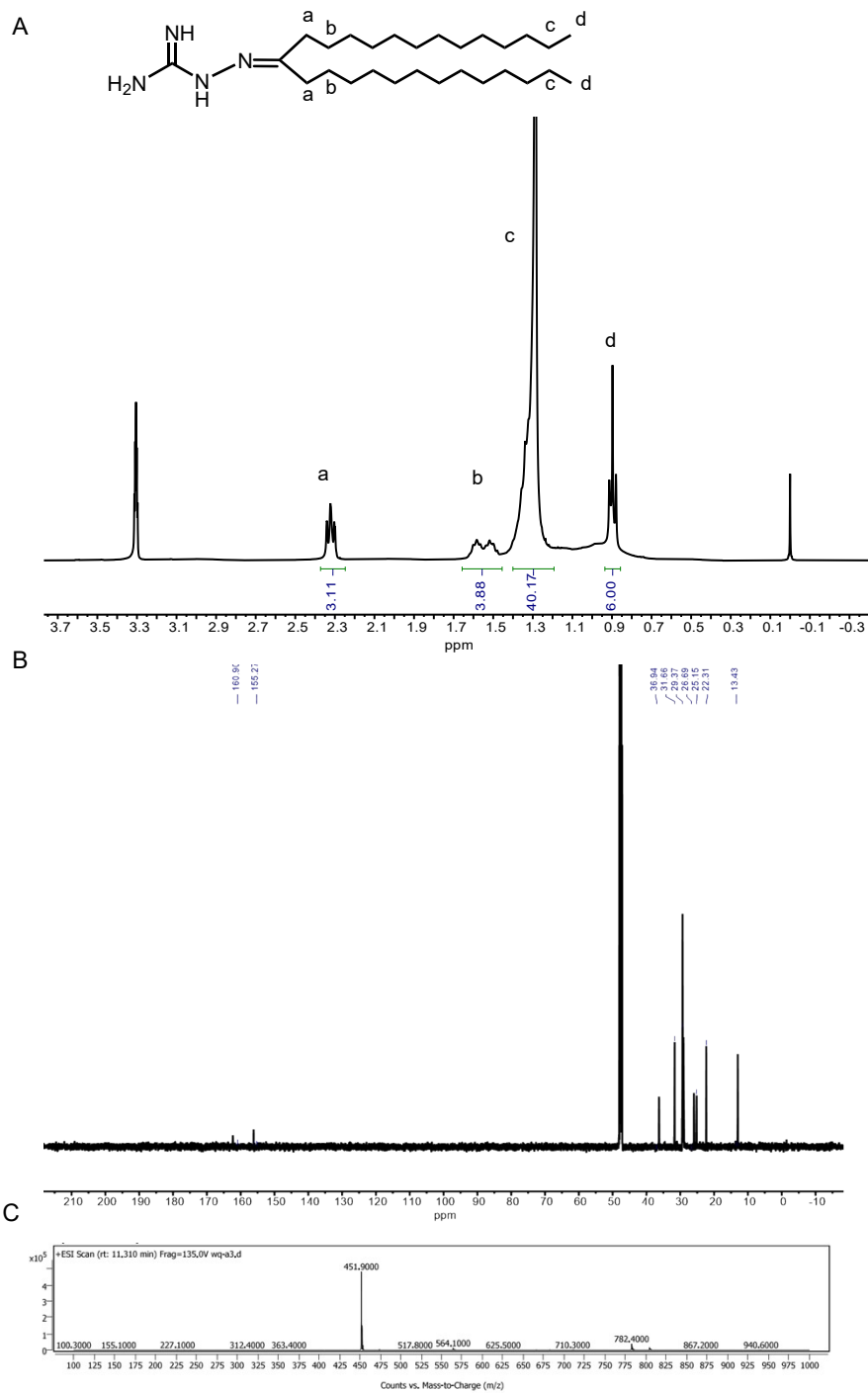


Figure S8 (A) The ^1H NMR spectrum of GL8 in CD_3OD . (B) The ^{13}C NMR spectrum of GL8 in CD_3OD .

(C) ESI-MS: m/z calculated for $\text{C}_{28}\text{H}_{58}\text{N}_4$ $[\text{M} + \text{H}]^+$: 450.80; found: 451.90.

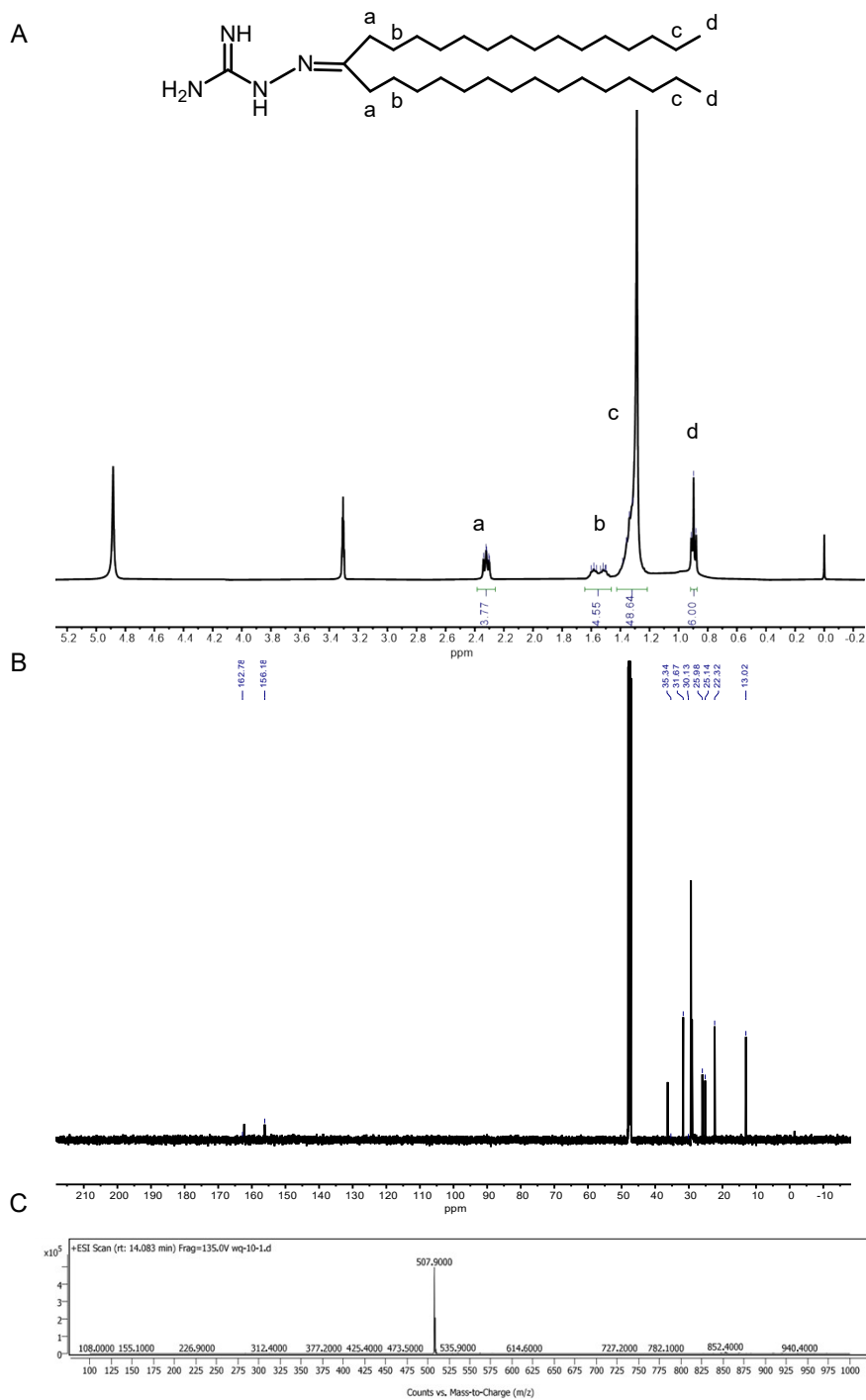


Figure S9 (A) The ^1H NMR spectrum of GL9 in CD_3OD . (B) The ^{13}C NMR spectrum of GL9 in CD_3OD . (C) ESI-MS: m/z calculated for $\text{C}_{32}\text{H}_{66}\text{N}_4$ $[\text{M} + \text{H}]^+$: 506.53; found: 507.9.

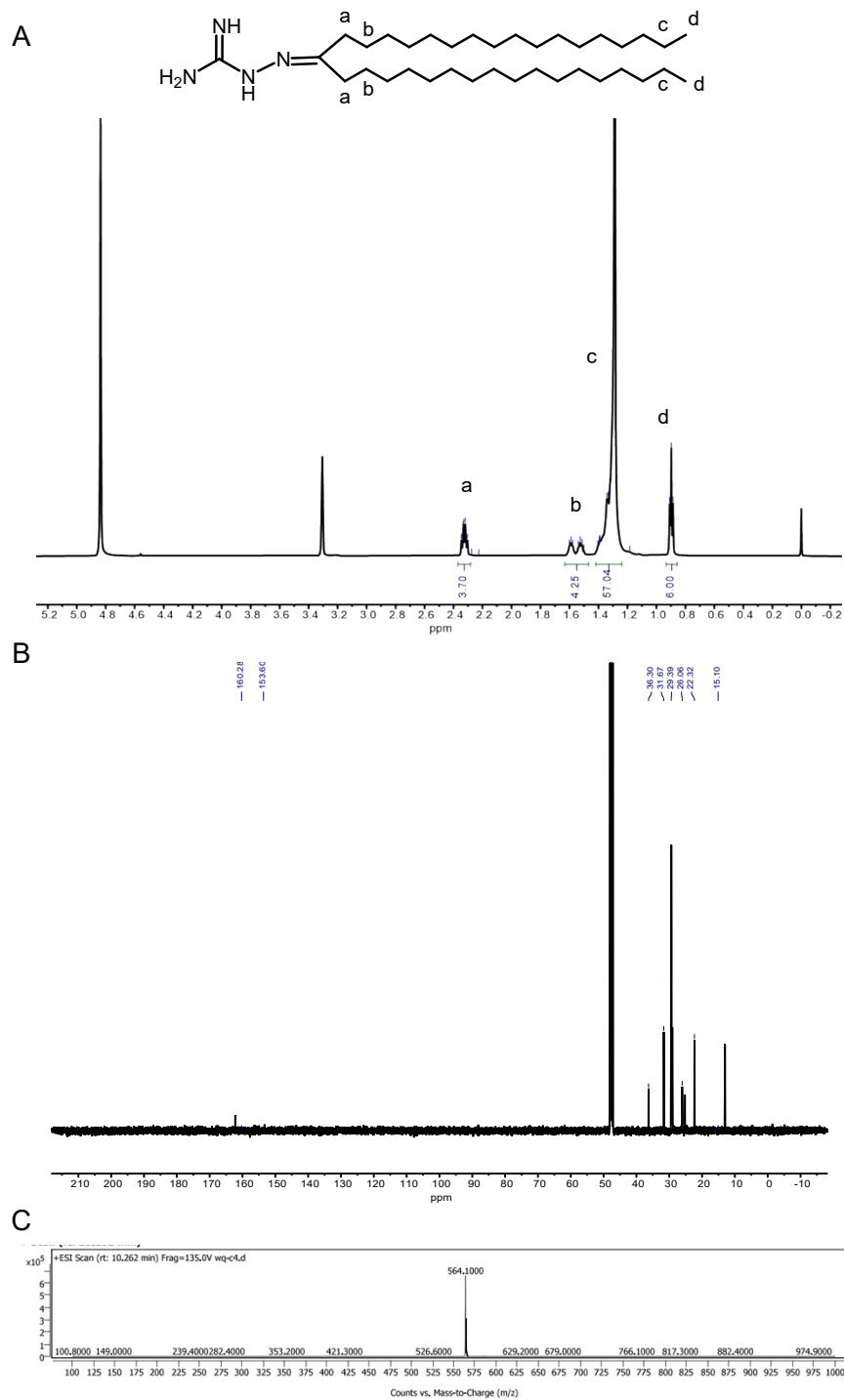


Figure S10 (A) The ^1H NMR spectrum of GL10 in CD_3OD . (B) The ^{13}C NMR spectrum of GL10 in CD_3OD . (C) ESI-MS: m/z calculated for $\text{C}_{36}\text{H}_{74}\text{N}_4$ $[\text{M} + \text{H}]^+$: 563.6; found: 564.1.

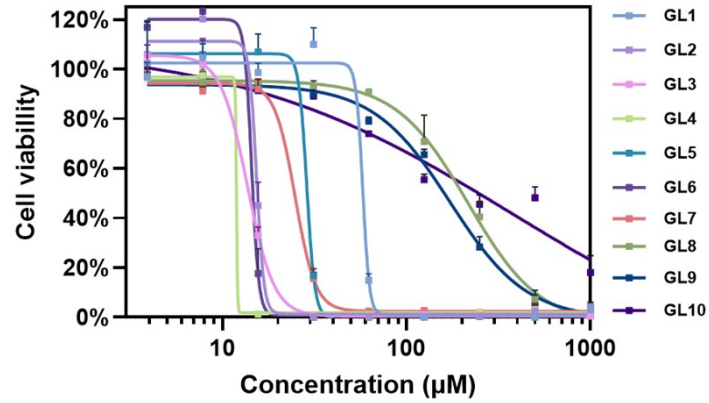


Figure S11 Cell viability curves of BHK-21 cells co-incubated with guanidinium lipids (GLs) for 24 h. Data represent the means \pm SD (n = 3).

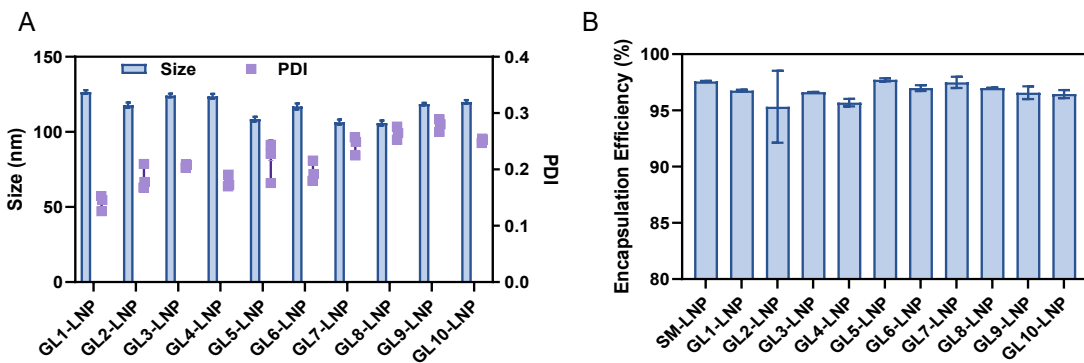


Figure S12 (A) The size and PDI of GL-LNP measured by dynamic laser scattering in PBS. (B) The encapsulation efficiency of GL-LNP. Data represent the means \pm SD (n = 3).

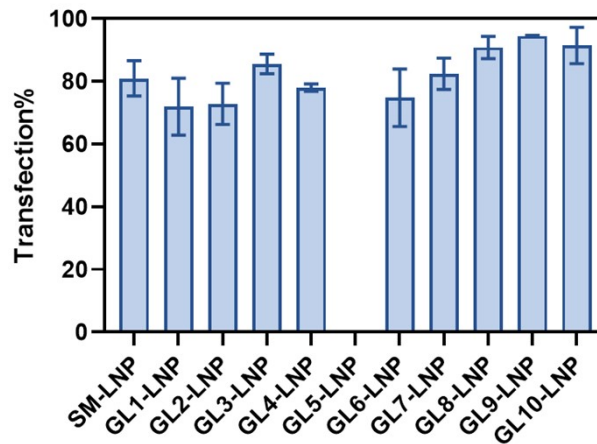


Figure S13 Transfection ratio of BHK-21 cells 24 h after transfection with the GL-LNP encapsulating EGFP mRNA (mRNA: 2 μ g/mL). Data represent the means \pm SD (n = 3).

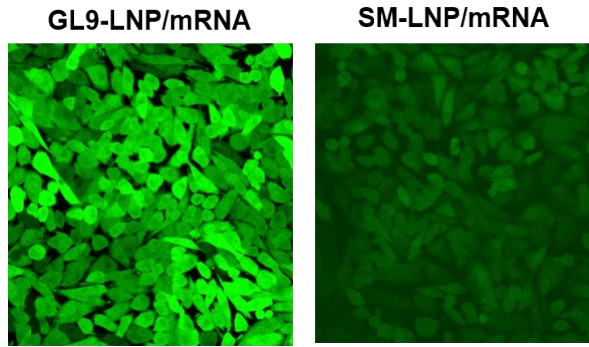


Figure S14 Confocal microscopy images of BHK cells 24 h after transfection with GL9-LNP or SM-LNP encapsulating EGFP mRNA (mRNA: 1 $\mu\text{g}/\text{mL}$).

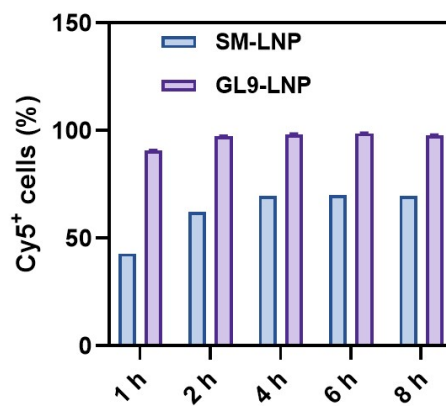


Figure S15 The proportion of Cy5+ cells in BHK-21 cells at different time points treated with LNP encapsulating Cy5-labeled mRNA (mRNA: 2 $\mu\text{g}/\text{mL}$). Data represent the means \pm SD (n = 3).

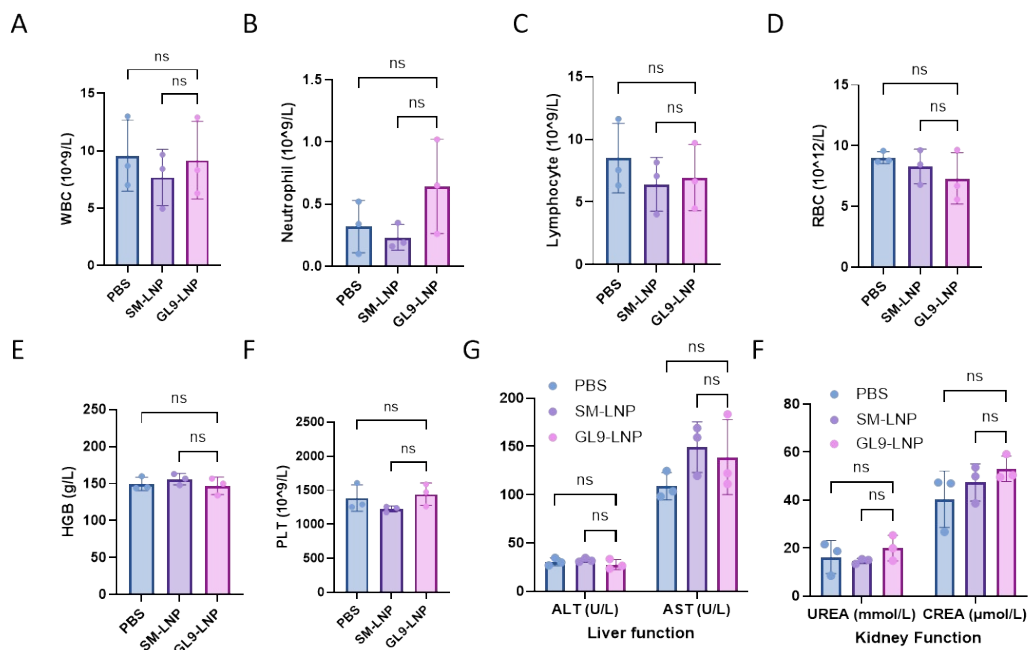


Figure S16 Routine blood tests, hepatic and renal function analysis of mice at 24 h after

intramuscular injection of SM-LNP or GL9-LNP (mRNA dose: 0.1 mg/kg). (A) White blood cell count (WBC); (B) Neutrophils; (C) Lymphocytes; (D) Red blood cell count (RBC); (E) Hemoglobin (HGB); (F) Platelets (PLT); (G) Hepatic function index: ALT and AST; (H) Renal function index: Urea and Creatinine. Data represent the means \pm SD (n = 3).

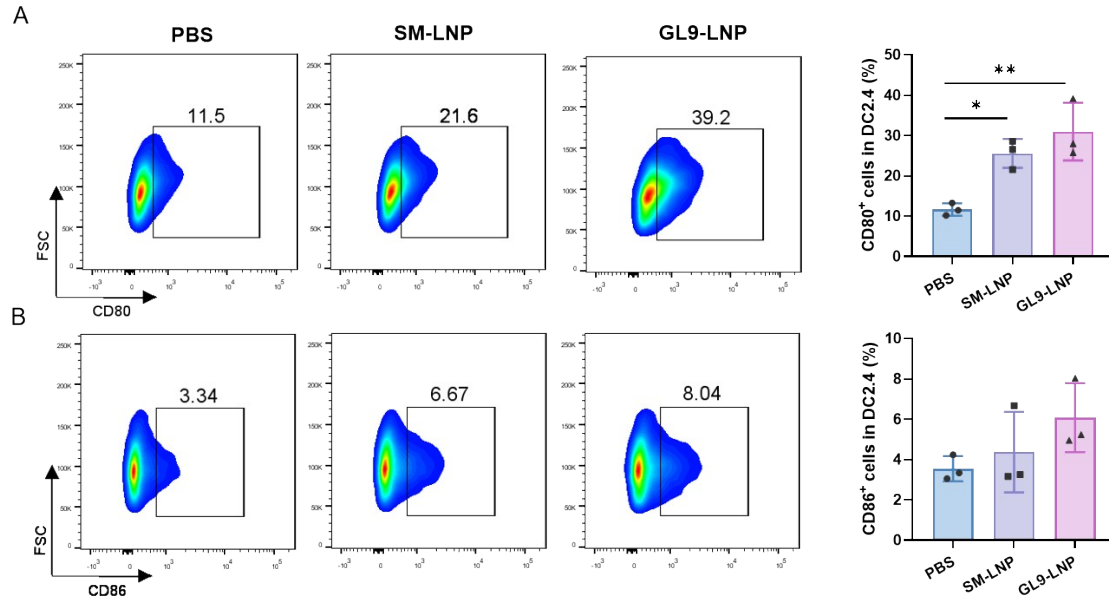


Figure S17 GL9-LNP stimulated DC2.4 Cell maturation in vitro. Representative flow cytometric analysis and quantification results of (A) CD80⁺ and (B) CD86⁺ cells in DC2.4 cells after treatment with SM-LNP or GL9-LNP (mRNA: 1 μ g/mL) for 24 h. Data represent the means \pm SD (n = 3). One-way ANOVA was used for the comparisons. * indicates a statistically significant difference between groups (ns, not significant; *p < 0.05; **p < 0.01).

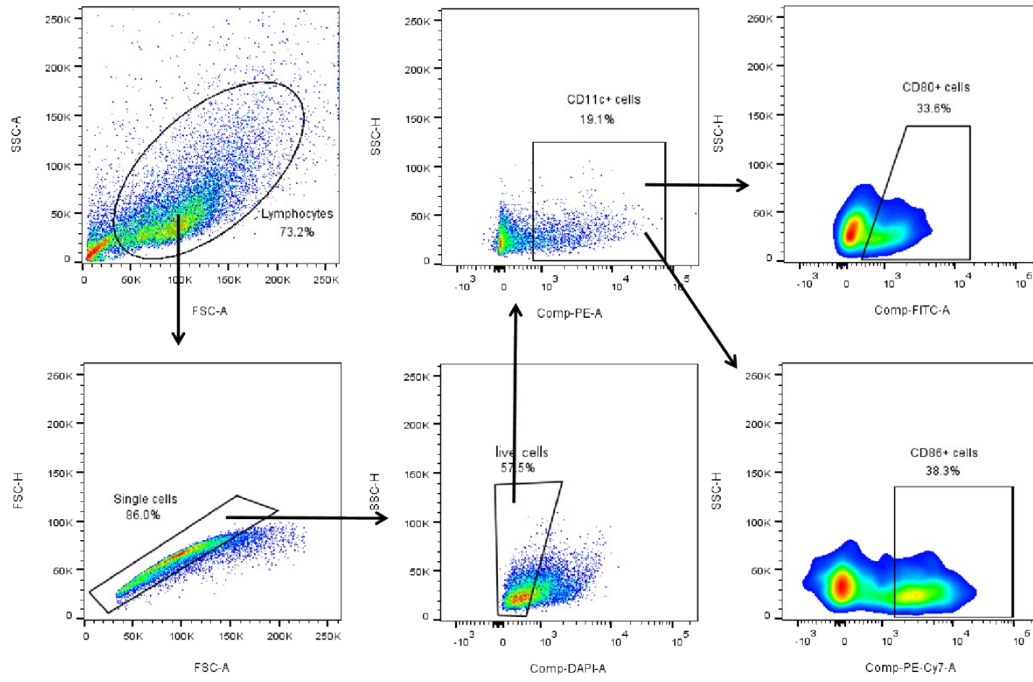


Figure S18 Representative flow cytometry gating strategies for experiments in Figure 6 and Figure S7.

Lipids	IC50 (μM)
GL1	57.9
GL2	15.3
GL3	13.7
GL4	11.9
GL5	28.7
GL6	14.4
GL7	24.9
GL8	172.5
GL9	216.2
GL10	378.3

Table S1 The IC50 values of the cytotoxicity curves for BHK-21 cells after treatment with GLs.